~~RESTRICTED~~ UNCLASSIFIED

ARL. LAB. Project No. MX 363
Contract No. W 33-038ac-4441
AAF MATERIEL COMMAND

Memorandum No. 2-2

THE DRAG OF STREAM-LINED BODIES

Louis G. Dunn

Copy No. ____

RESTRICTED
Classification ...
Authority Ltr TSPIN2C, 1 Dec 45
Date: JUL 2 1946 by 2.2 Nuclear (mn)

Louis G. Dunn, Associate
Chief Engineer, GALCIT
Project No. 1

for Clark B. Millikan

Th. von Kármán, Director
Guggenheim Aeronautical
Laboratory

JET PROPULSION LABORATORY
GALCIT
California Institute of Technology
November 10, 1944

UNCLASSIFIED ~~RESTRICTED~~

TABLE OF CONTENTS

	Page
INTRODUCTION	1
SKIN FRICTION DRAG OF STREAM-LINE BODIES	2
FORM OF PRESSURE DRAG OF STREAM-LINE BODIES	5
INTERFERENCE DRAG	7
EFFECT OF FINENESS RATIO ON DRAG	7
CAVITATION	9
CONCLUSIONS	11
REFERENCES	13
FIGURES 1 to 10	15 to 24

LIST OF FIGURES

Figure		Page
1	Skin Friction Drag Coefficient C_f of Stream-Line Bodies as a Function of Reynolds Number R	15
2	Drag Coefficient C_f as a Function of Reynolds Number for a Model of the R 101 Airship From Ref. 4	16
3	Effect of Fineness Ratio on Drag for Constant Diameter	17
4	Stream-Line Bodies: R 101, R 102, Body A and Body B . .	18
5	Bodies of Constant Volume Varying Fineness Ratio.	19
6	Variation of Diameter, Length and Area as a Function of Fineness Ratio	20
7	Drag as a Function of Fineness Ratio	21
8	Pressure Distribution Along Longitudinal Section Yaw Angle = 0° Body Without Fins MK 13	22
9	Pressure Distribution - Body B	23
10a	Fineness Ratio and Pressure Distribution - Body C	24
10b	Fineness Ratio and Pressure Distribution - Body D	24

THE DRAG OF STREAM-LINED BODIES

Introduction

In attempting to arrive at an optimum shape for the design of a high speed aircraft torpedo, a considerable number of factors must be taken into account, the following in particular require careful consideration:

1) The entry characteristics of the body.
2) The overall drag of the body -- including cavitation characteristics.
3) Stability during airflight and the underwater run.
4) The volume and linear dimensional requirements of the contents to be housed inside the body.
5) The overall dimensions as they effect launching aircraft.

It will, in general, not be possible to arrive at a shape which is an optimum for all the factors under consideration. For example, it is possible that a body shape giving the best entry characteristics may be completely incompatible with the other requirements. At present, the shape requirements for good entry are not as yet definitely known. However, it is clear that the nose shape, the mass moment of inertia and the overall length has a marked influence on the entry phase and the subsequent underwater path.

Sufficient information (see references) is available on the drag of stream-line bodies to allow a comparative study on the influence of the shape on the overall drag. The overall drag of a torpedo consists essentially of 1) skin friction drag of body and fins, 2) form or

pressure drag of body and fins, 3) interference drag between body and fins. In the following sections, the contribution of each to the overall drag will be separately discussed.

Skin Friction Drag of Stream-Lined Bodies

The discussion will be limited to stream-lined bodies which are solids of revolution whose generators consist of smooth continuous curves. An essential characteristic of such bodies is that separation of the flow does not occur except possibly near the extreme tail end. The boundary layer on a stream-line body resembles in many respects that on a flat plate in the direction of flow. Thus a laminar portion near the nose is succeeded by a transition to turbulence further aft. The transition from laminar to turbulent flow and also the position of transition varies with the Reynolds number R and with the turbulence in the main stream. An increase in Reynolds number or in turbulence will cause the transition point to move forward. For the turbulence present in an average wind tunnel (reference 2), the region of Reynolds number over which transition occurs lies between 1.5×10^6 and 10^7. Here the linear dimension on the Reynolds number corresponds to the axial length of the body.

In discussing the drag of stream-line bodies as measured in wind tunnels or water tunnels, three regions of the Reynolds number must be considered namely, a) small Reynolds numbers where the flow in the boundary layer is laminar, b) a transition region where over the forward portion the flow is laminar and over the aft portion turbulent, c) large Reynolds numbers where the boundary layer is turbulent over the entire length. The test data of figure 2, reproduced from reference 14, clearly illustrates these three regions. For R less than 1.5×10^6 the flow is laminar, between 1.5 and 7×10^6 the transition point moves

forward with a resulting increase in the drag coefficient. For R greater than 10^7 the entire boundary layer is turbulent and the drag coefficient decreases with increasing R.

These experimental results indicate clearly that a very wide variation in drag coefficient can be obtained depending on the state of the boundary layer. For most practical cases it will be of very little use to experiment with stream-line bodies unless R is sufficiently large to insure that substantially the whole boundary layer is turbulent. The full scale Reynolds number for the present hydrobomb is 10^8. At this Reynolds number, the existence of a laminar boundary layer over even a small fraction of the surface near the nose is extremely doubtful.

The similarity previously noted between the boundary layer on a flat plate and on a stream-lined body would lead one to expect that the drag coefficient of a stream-line body and a flat plate would not be markedly different at the same Reynolds number. Experimental results on the total drag of stream-line bodies (figure 4) have been collected from the references listed and are compared with the drag coefficient of a flat plate in figure 1. Only the data for test conditions which insured that all, or nearly all, of the boundary layer was turbulent are plotted in this figure. The drag coefficient of a flat plate when the boundary layer is entirely turbulent is given by the equation:

$$C_f = 0.455\ (\log_{10} R)^{-2.58}$$

and when the boundary layer is entirely laminar by

$$C_f = 1.328\ R^{-\frac{1}{2}}$$

The drag coefficient C_f is based on the total surface area.

The relative merits of stream-line bodies of different shape are generally estimated in terms of the drag coefficient K_d , where

$$K_d = \frac{\text{Drag}}{\frac{\rho}{2} v^2 (\text{volume})^{2/3}}$$

For bodies of the same fineness ratio the values of C_d can be directly compared because the ratio,

$$\frac{K_d}{C_f} = \frac{\text{Surface Area}}{(\text{volume})^{2/3}}$$

is essentially a constant. It is also clear that bodies of different fineness ratio will have different values of K_d even though C_f is a constant. For example, for bodies of the same shape and constant volume K_d will vary as the cube root of the fineness ratio. For this reason C_f was used to correlate the available experimental results.

It is seen (figure 1) that for stream-line bodies of approximately the same general shape, the values of drag coefficient are somewhat higher but very nearly parallel to the flat plate curve. This is true for both turbulent and laminar boundary layers, see figure 2 for laminar. Water tunnel results on the drag of the MK 13 torpedo are also plotted in figure 1. The drag coefficients for the MK 13 and for body B lies above the curve of the more conventional stream-line bodies. The higher values for the MK 13 correspond to total drag and total wetted surface (including tail surfaces); the lower values were obtained by subtracting the tail surface drag from the total drag. These results will be further discussed in the next section.

The difference in drag coefficient between stream-line bodies and a flat plate can be readily explained by the physical consideration that the average velocity over the surface of a stream-line body is greater than that over the surface of a flat plate in a stream having the same velocity at infinity. Theoretical calculations on the drag of stream-line bodies have been carried out for both laminar and turbulent

boundary layers, see reference 3 and 4. The theoretical results of reference 3 are in good agreement with experiment. The disadvantage of the theory is that it is quite laborious. As indicated above different curves will be obtained for bodies of markedly different shape because of the difference in the average velocity over the surface. In particular, it can be seen that the greater the fineness ratio (ratio of axial length to maximum diameter), the smaller will be the amount by which the curve for the stream-line body lies above that for the flat plate. This follows from the fact that as the fineness ratio increases the average velocity over the surface becomes more nearly equal to that over the flat plate.

The experimental results of figure 1 are of considerable practical value. They indicate that if, for any experiment the curve of drag coefficient versus Reynolds number falls near the curve for the flat plate in a turbulent flow one can be reasonably sure that the entire flow over the surface of the body is turbulent and the results will not be greatly affected by turbulence in the tunnel stream. Also for stream-line bodies of not too small a fineness ratio, the drag of the bare hull can be estimated from the experimental curve.

Form or Pressure Drag of Stream-Line Bodies

As previously stated, we are restricting ourselves to bodies for which separation does not occur and the drag of the body arises mainly from skin friction. However, there is usually some form drag resulting from the distribution of normal pressures over the surface. For most stream-lined bodies, the form drag is small, however, there are stream-line bodies for which it is appreciable despite the absence of separation. This will in general be true for bodies of small fineness ratio and those which are not too well stream-lined.

The pressure drag of stream-line bodies is generally obtained from an integration of the axial components of force acting over the surface of the body. This can be readily accomplished by plotting the experimentally observed pressure distribution as a function of the cross-sectional area from which the net resultant axial force can be obtained by graphical integration. A disadvantage of the method is, that the result is dependent on the difference between areas of the same order of magnitude.

Careful measurements on the stream-line bodies, R 101, R 102, R 33*and Body A, reference 5, 6 and 7, have lead to the conclusion that the pressure drag is either so small as to be not measurable or at most of the order of 4 to 6 per cent. Inasmuch as the MK 13 body is not of a highly stream-lined form, it is likely to exhibit a somewhat greater pressure drag. In reference 16 it is reported that the pressure drag as obtained from a graphical integration of the pressure distribution is about 12 1/2 per cent of the total drag.

Test on the bare hull of the MK 13 have indicated that over the range of Reynolds number, covered in the tests, the tail surfaces contribute about 12 per cent to the total drag. On this basis the upper drag curve for the MK 13, which is based on total drag and total wetted surface, figure 1, has been corrected to the lower curve based on bare hull drag and hull surface area. This curve is on the average 13 per cent higher than that for the stream-line bodies. This increase in drag is due mainly to pressure drag and possibly to a small extent to higher average velocities over the surface of the body. As previously noted, the stream-line bodies have pressure drags of possibly 3 to 4 per cent of the total drag. Thus the drag obtained by subtracting the

* The R 33 has a fineness ratio of 7.9:1

tail surface drag from the total drag gives a pressure drag of the same order of magnitude as that obtained from the pressure distribution.

Stream-line body B also indicates a higher drag coefficient based on total drag. The pressure drag for this body is reported to be approximately 27 per cent of the total drag, (reference 2). The curves of figure 2 indicate that this body has a drag coefficient about 20 per cent higher than the other stream-line bodies. These results show that for small fineness ratios the pressure drag increases rapidly and indicate an approach to the condition for separation caused by the rapid convergence of the after-body.

Interference Drag

Experimental data on interference drag is rather meager. In reference 20 are reported a series of tests on the measurement of the additional drag caused by tail surfaces on airship hulls. The general conclusions were that the additional drag for these particular tests was approximately equal to the drag of the fin surfaces and the interference drag was negligible. The tests on the MK 13 also indicate that for this particular body the interference drag must be very small.

Effect of Fineness Ratio on Drag

It seems quite likely that for stream-line bodies there is an optimum fineness ratio. If the fineness ratio is too small, the pressure drag will be large, on the other hand, once the fineness ratio is sufficiently large to ensure small pressure drag, any additional increase in length will merely increase the drag because of greater surface area.

Some experimental results on the effect of fineness ratio are given in reference 2 and are reproduced in figure 3. The test results were obtained on bodies having the same diameter but varying length. For

this reason, the results can be plotted as a function of C_d, the drag coefficient based on the cross-sectional area. These results point to a value of about 5 to 1 for the optimum fineness ratio at high Reynolds number. Since it is possible that, for the Reynolds numbers at which these tests were conducted, part of the boundary layer was turbulent and part laminar the result cannot be considered as conclusive.

The above type of variation in shape is not a logical one in the design of an aircraft torpedo because the volume changes very markedly for constant diameter and varying length. A more logical approach is to vary both the diameter and length and keep the volume constant. The drag can be calculated using the experimental results of figure 1 and relative merits of the various bodies can then be estimated in terms of K_d or total drag for a given velocity, which is the usual method employed in comparing airship shapes. Some calculations have been carried out for a series of shapes of the type indicated in figure 5. The shape of fineness ratio 5 was taken as the basic shape and by multiplying the ordinate and abscissa values by suitable constants other shapes all having the same volume were obtained. The variation of diameter, length and surface area as a function of fineness ratio is shown in figure 6. The basic equation for these shapes is discussed in the next section.

For fineness ratios of 5 and greater, the bare hull drag at 70 mph, figure 7, was calculated by using drag coefficients corresponding to the experimental C_f curve of figure 1. For fineness ratios less than 5 the drag is uncertain because of form drag. At fineness ratio of 3 the form drag is of the order of 27 per cent of the total drag and at 1 (sphere) the total drag is approximately 15 times greater than for a fineness ratio of 5.

The additional drag due to the tail surfaces is only a very rough approximation and was obtained in the following way. At a Reynolds number of 3.5×10^6 the tail surface drag of the MK 13 was reported as

12 per cent of the total drag. Hence, based on the cross-section area of the body the effective drag coefficient of the tail surfaces would be .015. Assuming the tail surface drag to be pressure drag then the drag coefficient would not be effected by Reynolds number. On this bases the tail surface drag at 70 mph would be 430 lbs. If it is further assumed that the tail surface drag is the same for bodies of different fineness ratio, then the total drag as a function of fineness ratio can be estimated and is shown in figure 7. It is felt that tail surfaces could be designed having a lower drag than that of the MK 13.

Cavitation

In underwater operation cavitation arises when the normal pressure on the surface is equal to or less than the vapor pressure of the water. Since the drag will probably increase rapidly as cavitation becomes fully developed the body shape of a high speed torpedo will be largely determined by its cavitation characteristics.

It is safe to conclude that a body shape which does not cavitate below 70 mph at, say, 15 feet submergence will also fulfill the requirements of low drag. It is to be noted that the drag coefficient for the R 101 shape is, within the experimental scatter, the same as that for body A which has a very much blunter nose shape.

In connection with the influence of shape on cavitation it is of interest to compare the pressure distribution on four bodies of different shape. Figure 8 and 9 give the pressure distribution over the MK 13 body and over body B repectively. Figure 10a and 10b give the pressure distribution over bodies C and D. These latter two stream-line bodies were investigated by Miss Lyon (Cf reference 11) in connection with the design of the R 100 airship. Body C is described by an equation of the form:

$$Z^2 = 1.23935\ (S - S^2 - S^3 + S^4)$$

and body D by

$$Z^2 = 2.3390\ S - 9.0022\ S^2 + 17.8238\ S^3 - 17.6885\ S^4 + 6.5279\ S^5$$

where $S = \frac{x}{L}$ (L = length, x = distance from nose)

$Z = \frac{y}{d}$ (d = diameter, y = diameter of circumscribing circle)

The above expressions were derived from the general equation

$$Z^2 = as + bs^2 + cs^3 + \text{-------} + ks^n + \text{----------}$$

which satisfies the condition that Z = 0 when S = 0. If for example five terms are used the boundary conditions are:

$Z = 0$	when	$S = 1$
$Z = 0.5$	when	$\frac{dZ}{dS} = 0$
$Z = S_m$	when	$\frac{dZ}{dS} = 0$
$\int_0^1 Z^2\, dS = \frac{K_b}{4}$		
$Z = K_1$	when	$S = K_2$

where S_m is the desired position of the maximum diameter and K_b is the block coefficient (ratio of the volume to the volume of the circumscribing cylinder). The last boundary condition is used to vary the bluntness of the nose. For body D, Z = 0.4 when S = 0.1, S_m = 0.4 and K_b = 0.7. The body shapes of figure 5 were determined from the equation of body D.

These shapes indicate that if the ordinate and abscissa is multiplied by appropriate constants to give larger fineness ratios, the nose shape becomes more pointed as the fineness ratio increases. By appropriate changes in the boundary conditions, blunter nose shapes can be obtained.

The pressure distribution is generally given in the ratio of

$$\frac{P - P_o}{\frac{\rho}{2} V_o^2}$$

where P is the normal pressure at the surface of the body in lbs/sq in. and P_o and V_o are, the free stream pressure and velocity respectively. Noting that for cavitation to occur P must equal the vapor pressure P_v it follows by definition that the cavitation parameter K is given by

$$\frac{P - P_o}{\frac{\rho}{2} V_o^2} = \frac{P_v - P_o}{\frac{\rho}{2} V_o^2} = -K$$

For a given fluid and submergence $P_v - P_o$ = constant and the dynamic pressure $\frac{V_o^2}{2}$ is proportional to 1/K. For a particular shape the minimum of the pressure ratio $(P_v - P_o) / \frac{\rho}{2} V_o^2$ corresponds numerically to its cavitation parameter. The pressure distribution also indicates the region over which incipient cavitation occurs. From the pressure distribution curves, figure 8, 9, 10a and 10b, it is seen that the incipient cavitation parameter for the MK 13 is 0.78, for body B it is 0.191, for body C it is 0.157 and for body D it is 0.23. The nose shape of body B is a 2.54:1 ellipse.

Conclusions

The experimental results and calculations indicate that for drag the optimum fineness ratio is close to 5:1 and that the increase in drag with increasing fineness ratio is relatively small. Figure 7 indicates that increasing the fineness ratio from 5 to 7.5 increases the total drag from 1830 to 1970 lbs, or 7.7 per cent. It is clear, therefore, that if any of the factors previously listed make it desirable to use a fineness ratio greater than 5:1 the increase in drag will not be excessive.

For a high speed torpedo the shape will be determined by cavitation considerations. By carefull design, shapes having a high volume efficiency can be obtained without markedly decreasing the cavitation resistance of the body. For example, body C will start to cavitate at 94 mph at a 15 feet submergence and body D at 79 mph at the same depth. The volume of body D is 21 per cent greater than that of body C for the same fineness ratio. The bare hull drag is about the same.

REFERENCES

(1) S. Goldstein, "Modern Developments in Fluid Dynamics," Vol. I, (1938)

(2) S. Goldstein, "Modern Developments in Fluid Dynamics," Vol. II, (1938)

(3) C. B. Millikan, "The boundary Layer and Skin Friction for a Figure of Revolution," Applied Mechanics Section, A.S.M.E. (1932)

(4) H. L. Dryden and A. M. Kuethe, "Effect of Turbulence in Wind Tunnel Measurements," N.A.C.A. Rep. No. 342, (1929)

(5) R. Jones and D. H. Williams, "The Distribution of Pressure Over the Surface of Airship Model U.721 Together With a Comparison With the Pressure Over Spheroids," R. and M., 600, (1919)

(6) R. Jones and A. H. Bell, "The Pressure Distribution Over a Model of the Hull of Airship R33," R. and M., No. 801, (1922)

(7) R. Jones and A. H. Bell, "The Distribution of Pressure Over the Hull and Fins of a Model of the Rigid Airship R.101, and a Determination of the Hinge Moments on the Control Surfaces," R. and M., 1169 (1927)

(8) L.F.G. Simmons, "Experiments Relating to the Flow in the Boundary Layer of an Airship Model," R. and M., no. 1268 (1929)

(9) E. Ower and C. T. Hutton, "Investigation of the Boundary Layers and the Drags of Two Streamline Bodies," R. and M., 1271 (1929)

(10) E. Ower and C. T. Hutton, "The Drag of Small Streamline Bodies," R. and M., 1409 (1931)

(11) H. M. Lyon, "Effect of Turbulence on Drag of Airship Models," R. and M., 1511 (1932)

(12) L.F.G. Simmons and A.F.C. Brown, "Experimental Investigation of Boundary Layer Flow," R. and M., 1547 (1934)

(13) H. M. Lyon, "Flow in the Boundary Layer of Streamline Bodies," R. and M., 1622 (1934)

(14) R. Jones and D. H. Williams, "Tests on Two Streamline Bodies in the Compressed Air Tunnel," R. and M., 1710 (1936)

(15) R. T. Knapp, "Water Tunnel Tests of the MK 13-1, MK 13-2 and MK 13-2A Torpedoes," HML Rep. No. ND-15 (1943)

(16) R. T. Knapp, "Pressure Distribution Measurements on the MK 13-1, 13-2 and 13-2A Torpedoes," HML Rep. No. ND-15.3 (1944)

(17) C.N.H. Lock and F. C. Johansen, "Drag and Pressure-Distribution Experiments on Two Pairs of Stream-Line Bodies," R. and M., 1452 (1933)

(18) H. L. Dryden, "Reduction of Turbulence in Wind Tunnels," N.A.C.A. Rep. No. 392 (1931)

(19) H. B. Freeman, "Measurements of Flow in the Boundary Layer of a 1/40-Scale Model of the U.S. Airship 'Akron", N.A.C.A. Rep. No. 430 (1932)

(20) I. H. Abbott, "The Drag of Two Streamline Bodies as Affected by Protuberances and Appendages," N.A.C.A. Rep. No. 451 (1932)

DIETERICH POST ... NO. 7123 LOGARITHMIC 2 CYCLES BY 2 CYCLES
PRINTED IN U.S.A. ON CLEARPRINT TECHNICAL PAPER NO 1000H

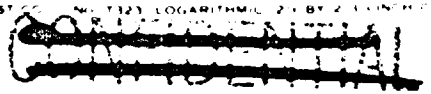

ARM. LAB. Proj. MX363
JPL-CALCIT
Memorandum No. 2-2
Page 15
Fig 1
UNCLASSIFIED

MK 13 - WITH FINS

MK 13 CORRECTED FOR FIN DRAG

FLAT PLATE - TURBULENT

C_f

.006
.005
.004
.003
.002
.001
.0008
.0006
.0004
.0002

SYMBOL	BODY	REF.
⊙	R101	14
△	R102	14
▽	A	9
□	B	9
×	R33	2
•	MK13	15

SKIN FRICTION DRAG COEFFICIENT C_f OF STREAMLINE-BODIES AS A FUNCTION OF REYNOLDS NUMBER - R

$$R = \frac{VL}{\nu}, \quad C_f = \frac{DRAG}{\rho/2 V^2 S}$$

V = VELOCITY IN FT/SEC L = TOTAL LENGTH IN FT

S = SURFACE AREA IN FT^2 ν = KINEMATIC VISCOSITY

ρ = DENSITY IN SLUGS/FT^3

10^6 2 4 6 8 10^7 2 4 6 8 10^8 2

REYNOLDS NUMBER - R →

FIG. 1

DIETERICH POST CO. No. T323 LOGARITHMIC 2½ BY 2 3 INCH CYCLES
PRINTED IN U.S.A. ON CLEARPRINT TECHNICAL PAPER NO. 1000H

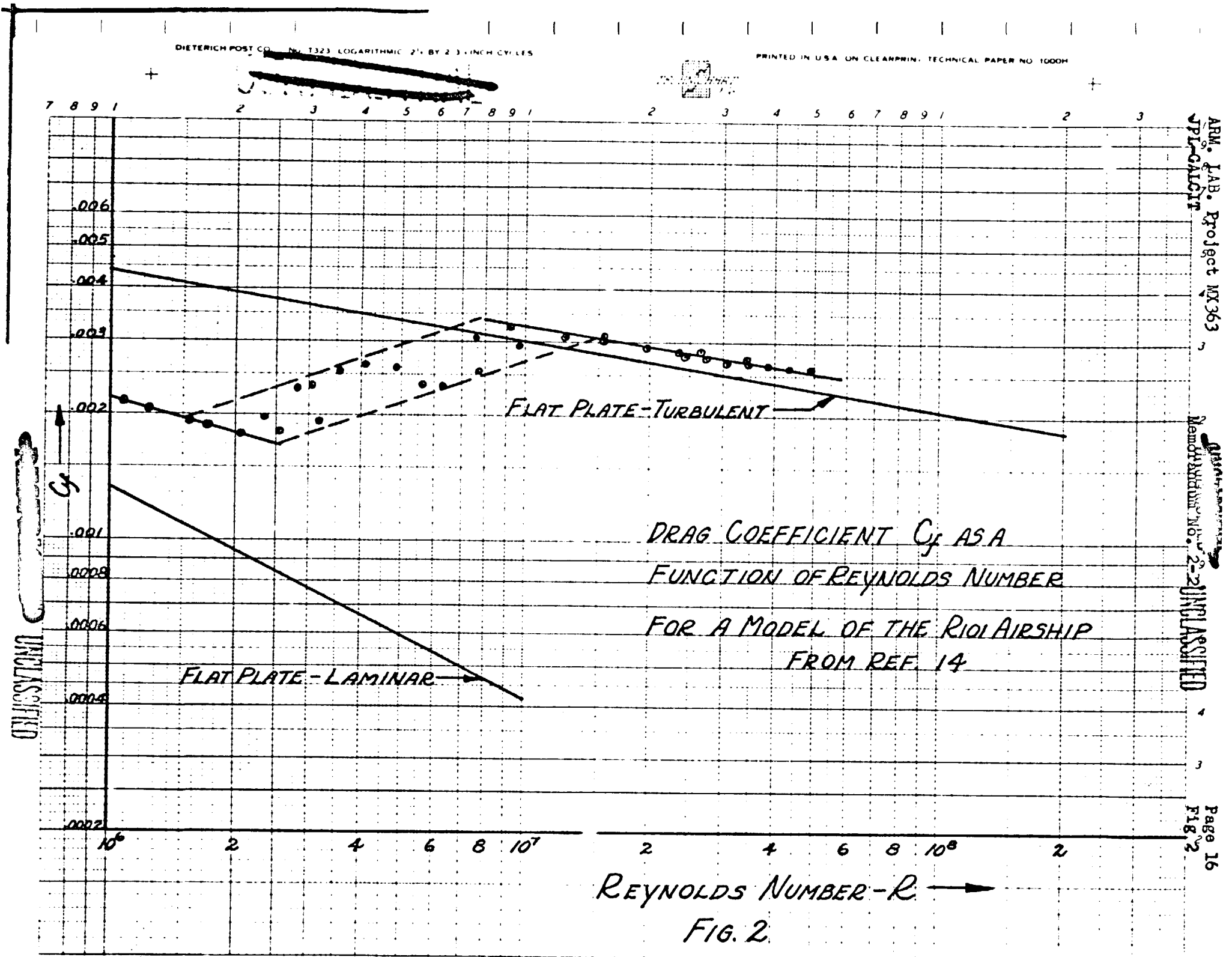

DRAG COEFFICIENT C_f AS A FUNCTION OF REYNOLDS NUMBER FOR A MODEL OF THE RIOI AIRSHIP FROM REF. 14

FIG. 2

UNCLASSIFIED
ARM. LAB. Project MX363
JPL-CALCIT
Memorandum No. 2-22
UNCLASSIFIED

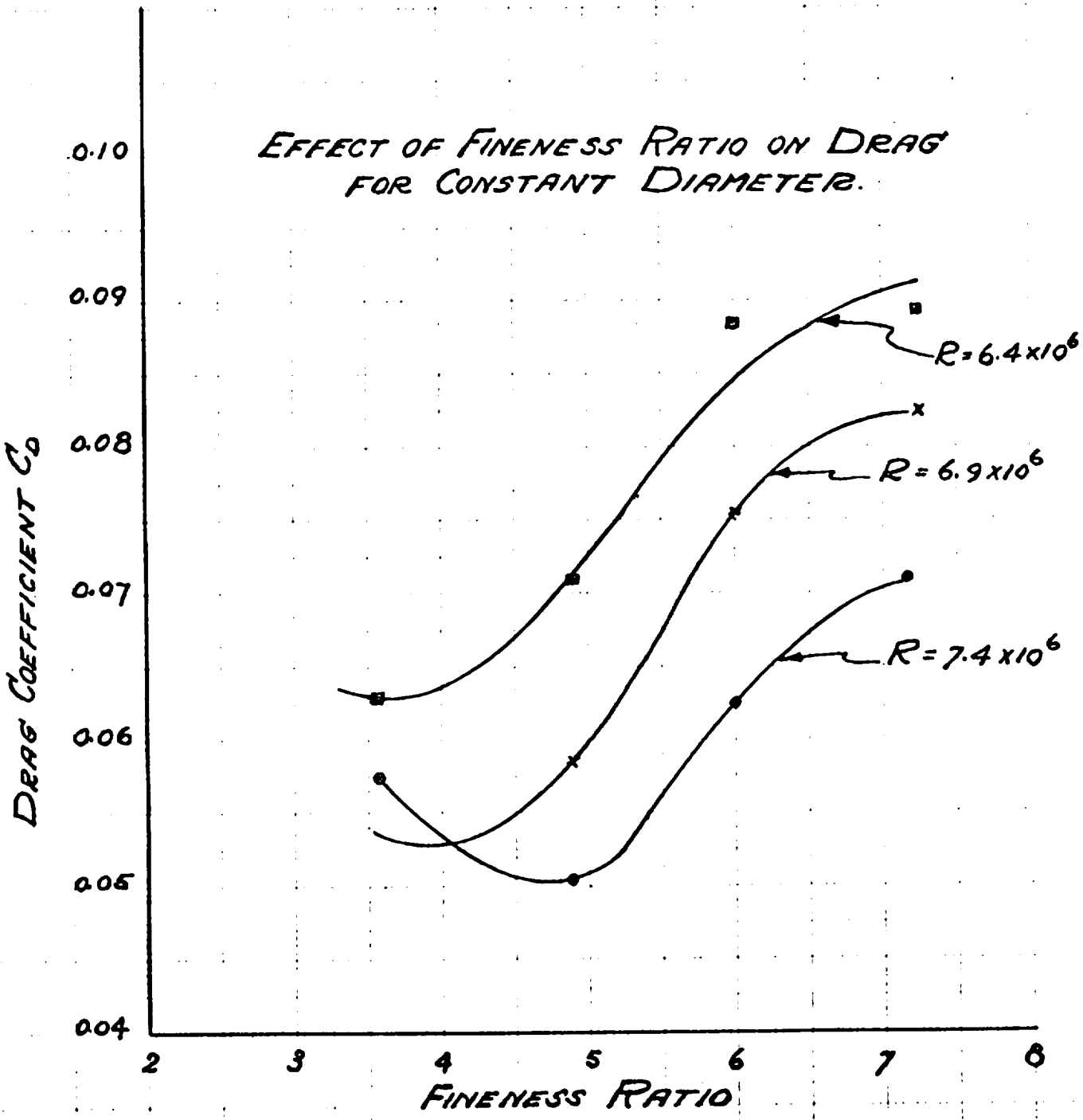
EFFECT OF FINENESS RATIO ON DRAG FOR CONSTANT DIAMETER.
DRAG COEFFICIENT C_D
0.10
0.09
0.08
0.07
0.06
0.05
0.04
2
3
4
5
6
7
8
FINENESS RATIO
R = 6.4 x 10^6
R = 6.9 x 10^6
R = 7.4 x 10^6

FIG. 3

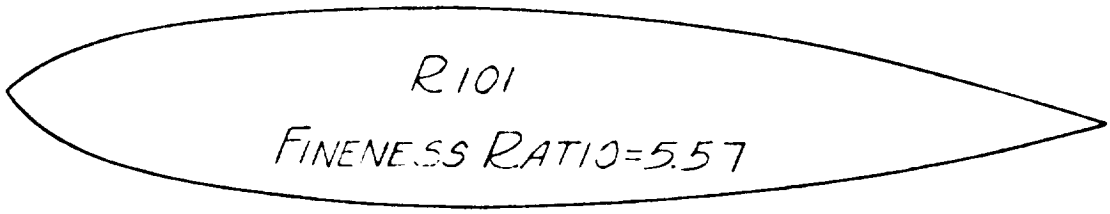
R101
FINENESS RATIO=5.57

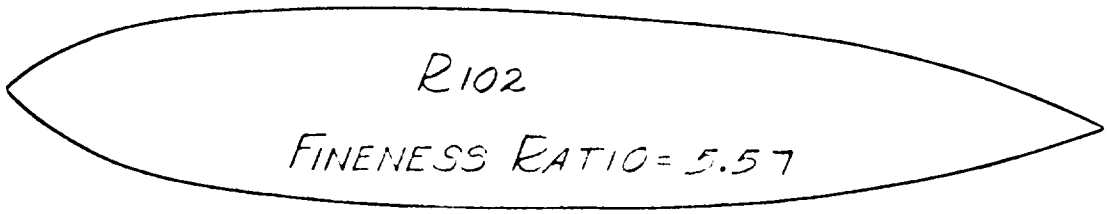
R102
FINENESS RATIO=5.57

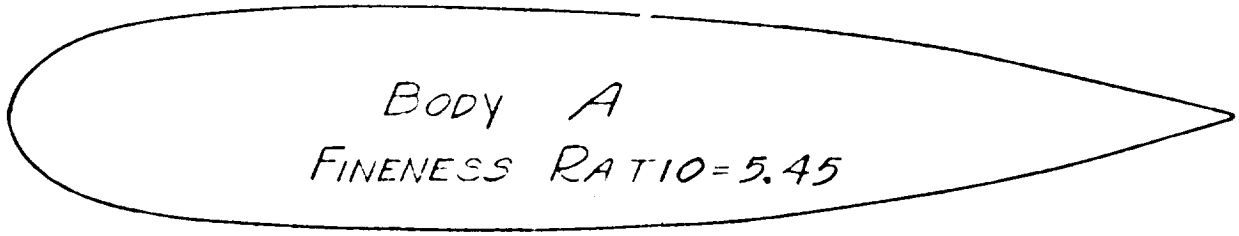
BODY A
FINENESS RATIO=5.45

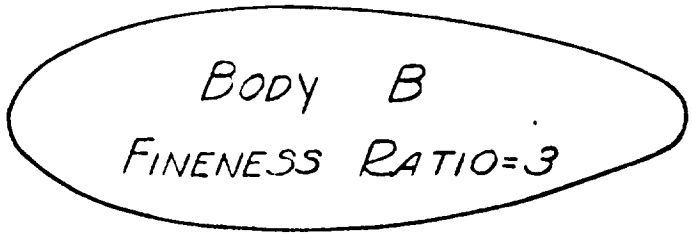
BODY B
FINENESS RATIO=3

FIG. 4.

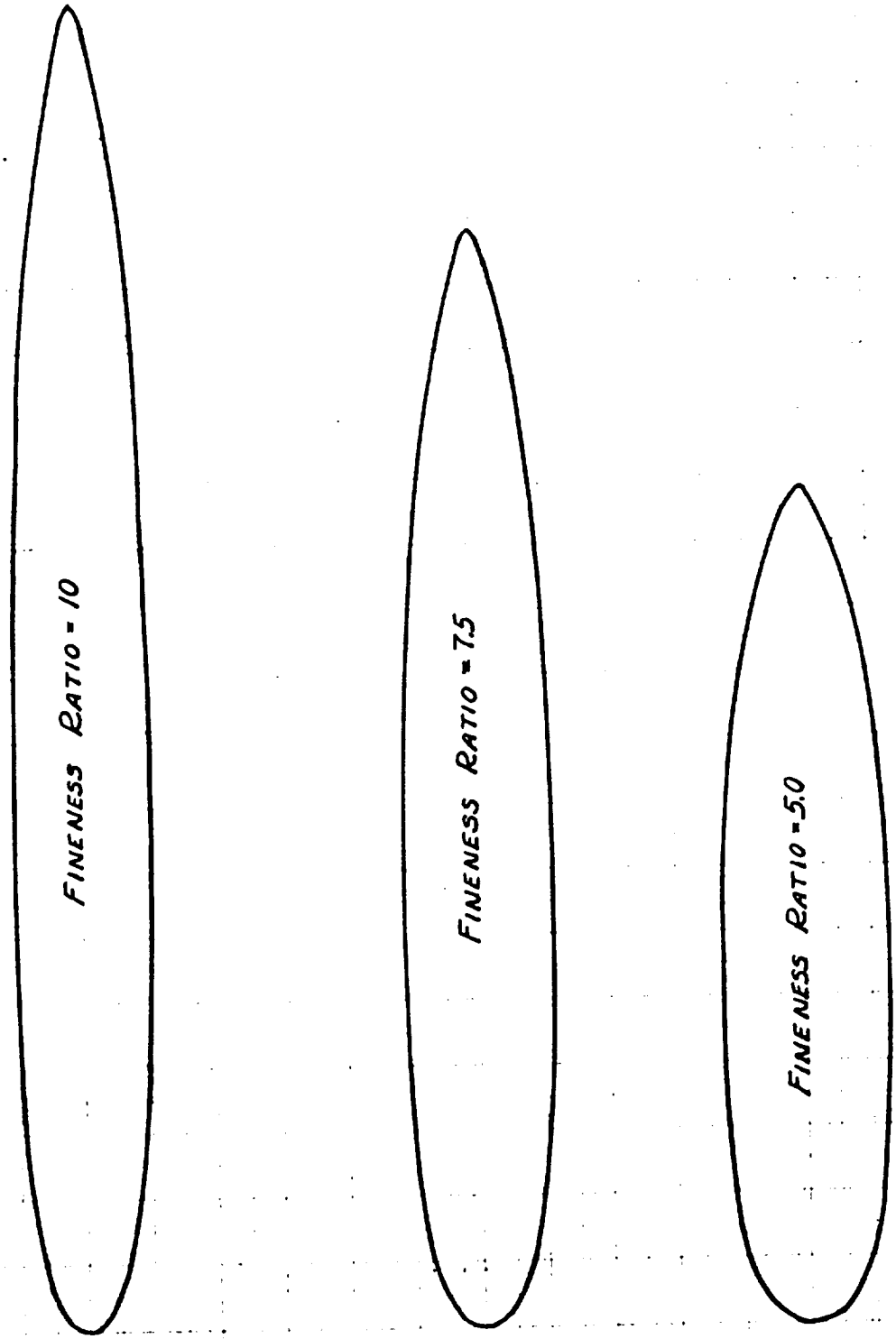

FIG. 5

BODIES OF CONSTANT VOLUME
VARYING FINENESS RATIO -

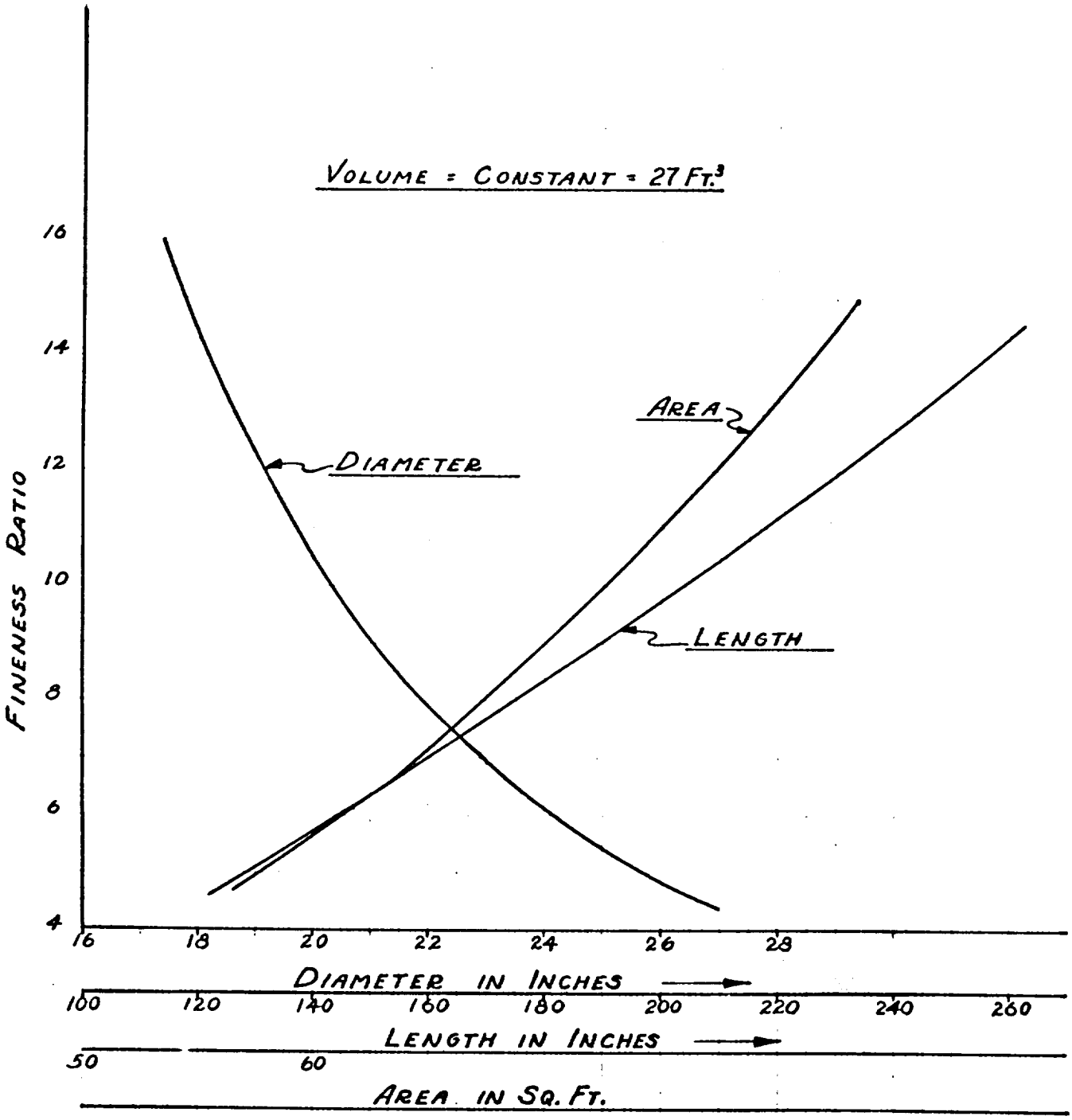
VOLUME = CONSTANT = 27 FT.³
FINENESS RATIO
16
14
12
10
8
6
4
DIAMETER
AREA
LENGTH
16
18
20
22
24
26
28
DIAMETER IN INCHES
100
120
140
160
180
200
220
240
260
LENGTH IN INCHES
50
60
AREA IN SQ. FT.

FIG: 6

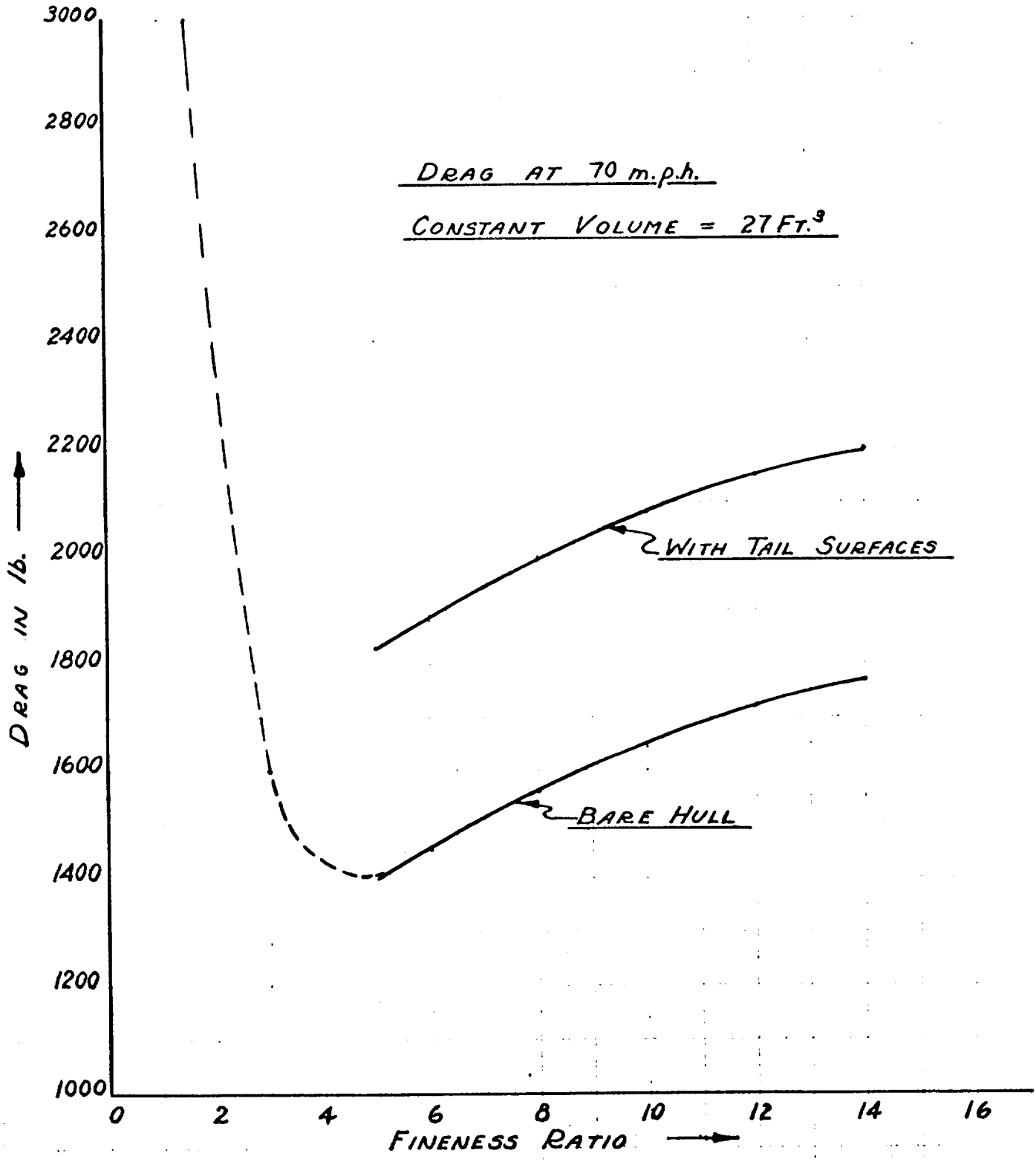
DRAG AT 70 m.p.h.
CONSTANT VOLUME = 27 FT.³
WITH TAIL SURFACES
BARE HULL
DRAG IN lb.
FINENESS RATIO
3000
2800
2600
2400
2200
2000
1800
1600
1400
1200
1000
0
2
4
6
8
10
12
14
16

FIG:7

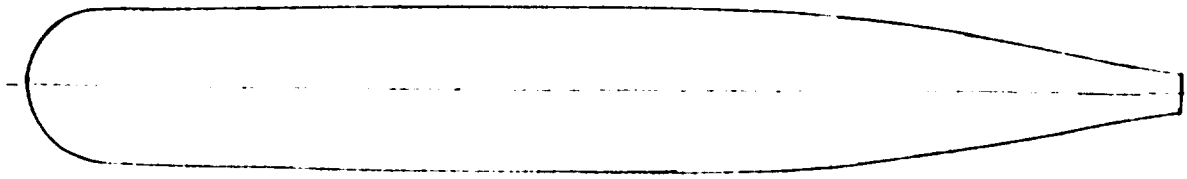

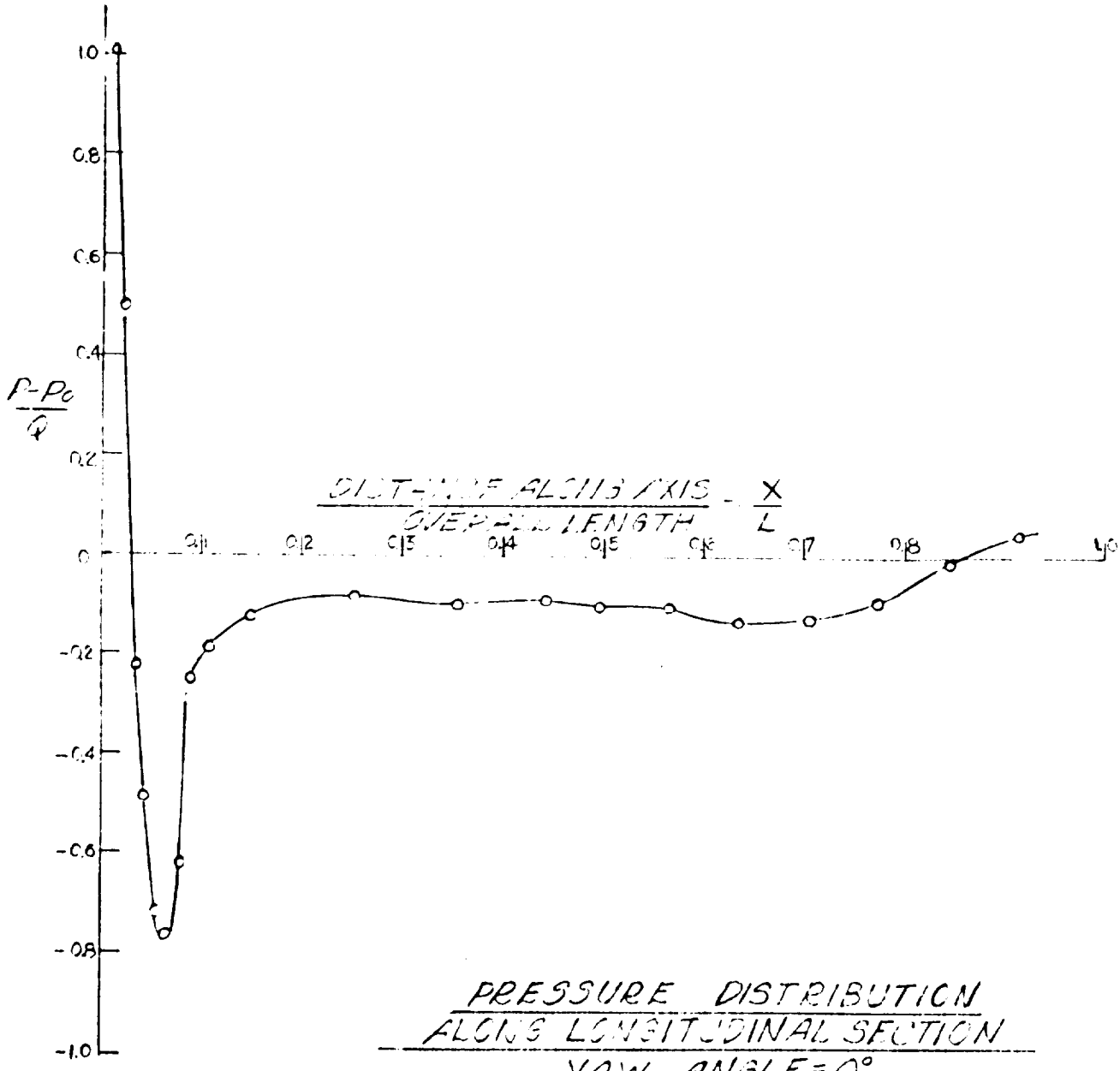

PRESSURE DISTRIBUTION
ALONG LONGITUDINAL SECTION
YAW ANGLE = 0°

BODY WITHOUT FINS

MK 13

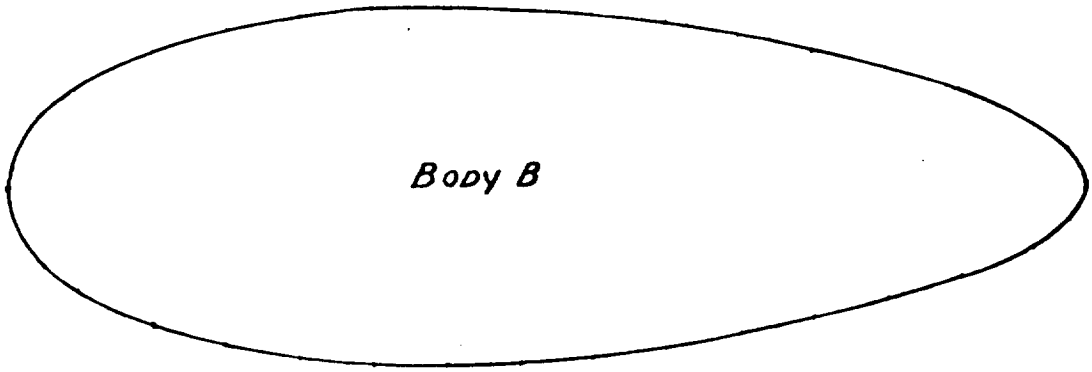
Body B

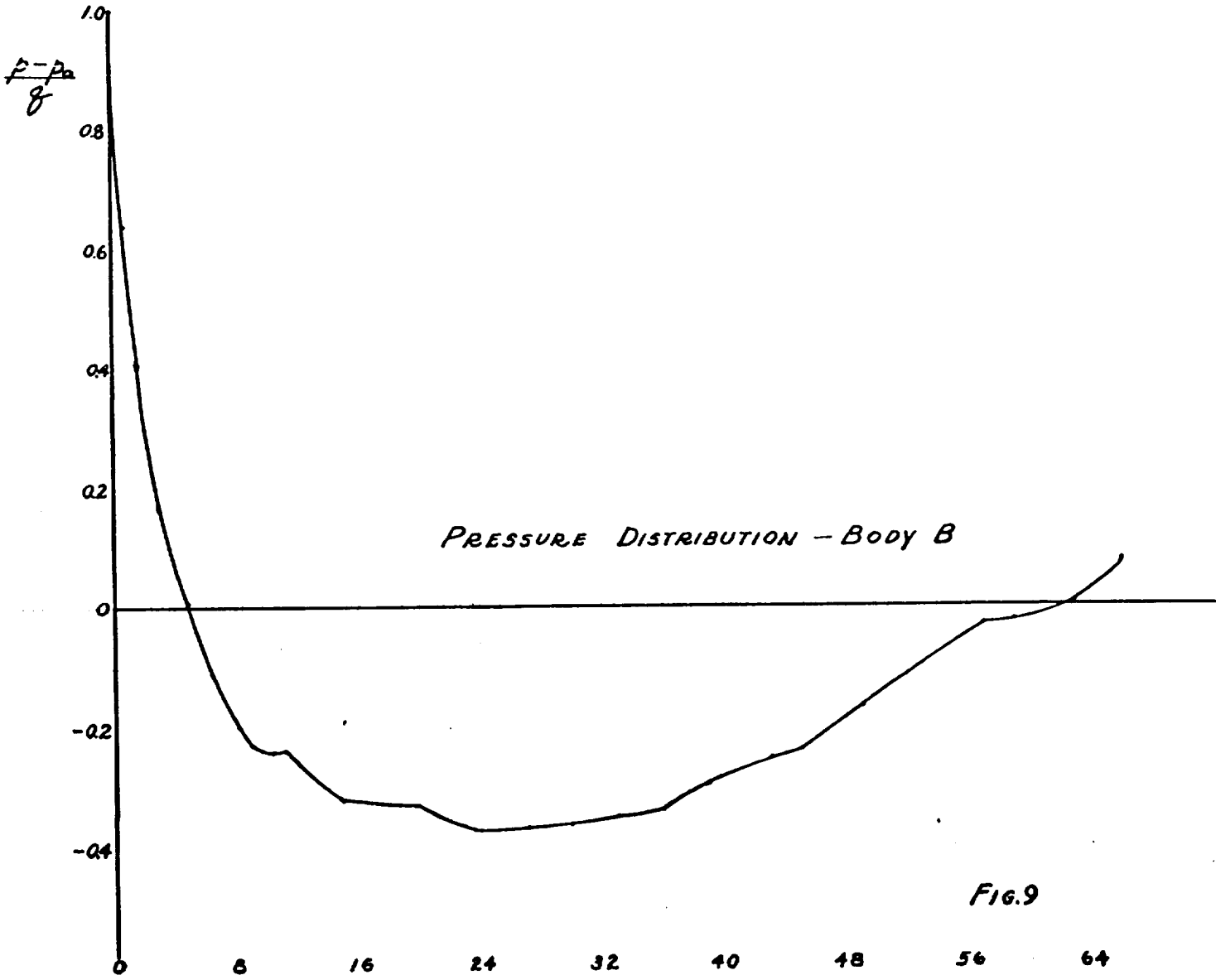
1.0
$\frac{p-p_a}{q}$
0.8
0.6
0.4
0.2
0
-0.2
-0.4
0
8
16
24
32
40
48
56
64
Pressure Distribution – Body B

Fig.9

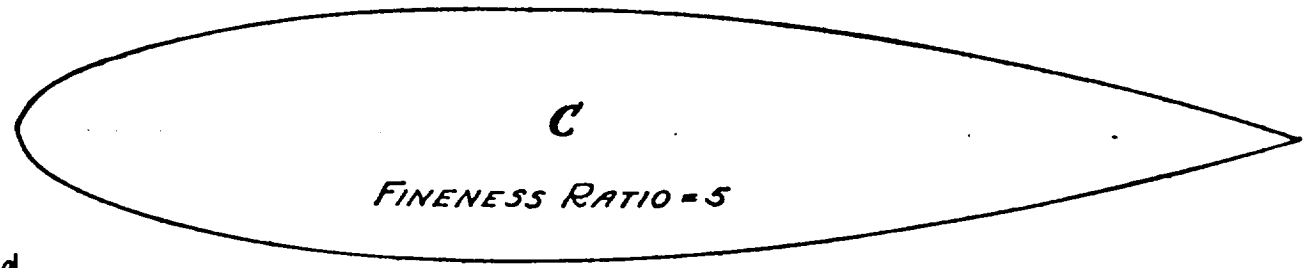

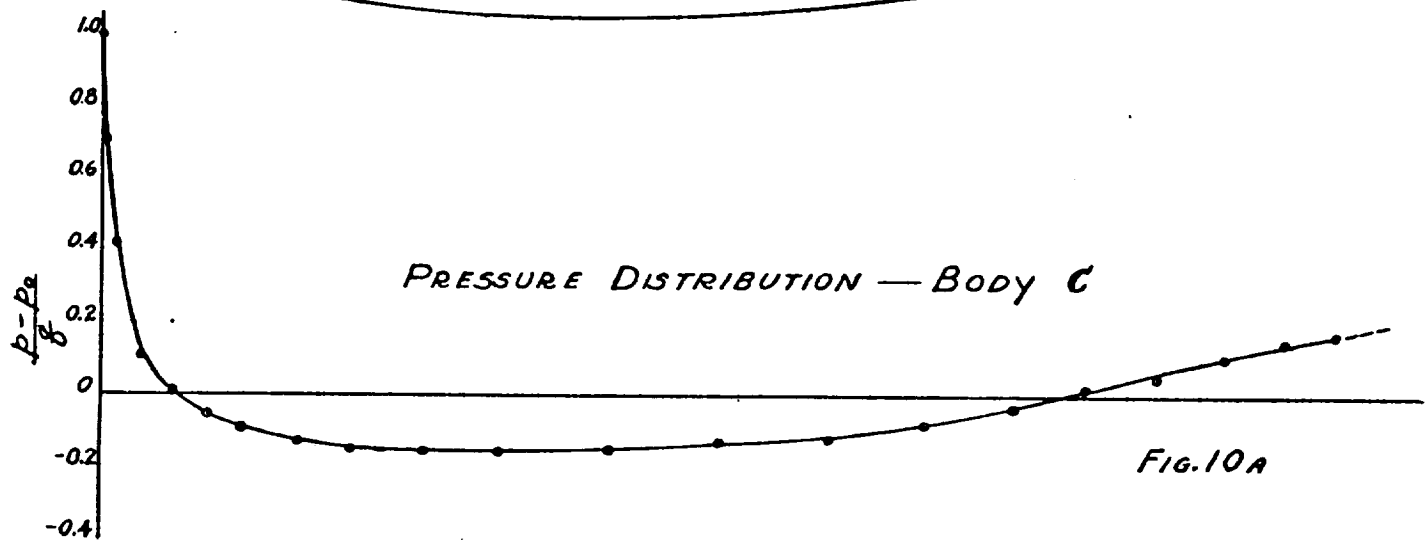

FIG. 10A

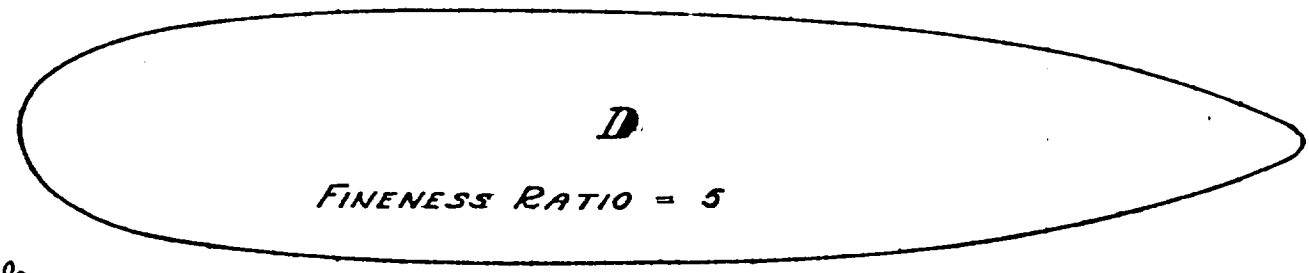

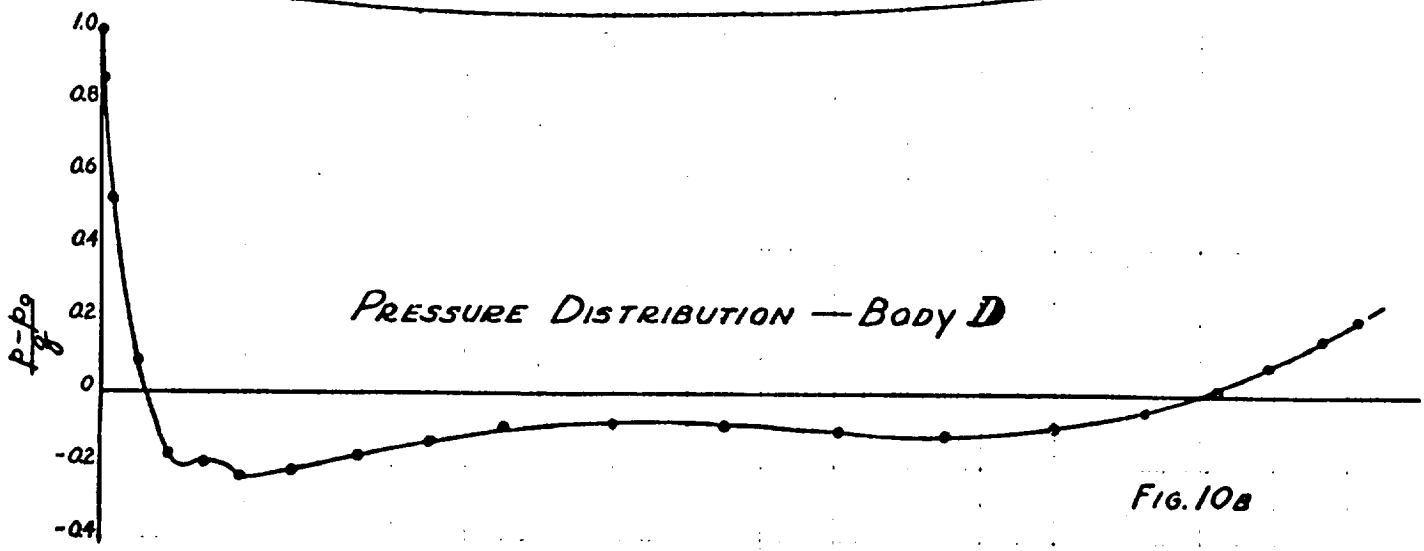

FIG. 10B

INITIAL DISTRIBUTION OF COPIES OF THIS REPORT

Nos. 1-4, Inclusion, to Director, Army Air Forces, Air Technical Service Command, Wright Field, Dayton, Ohio. (Armament Laboratory)

No. 5 to Colonel W. H. Joiner, War Department Liaison Office, California Institute of Technology.

No. 6 to Dr. Theodore von Karman, California Institute of Technology.

No. 7 to Dr. C. B. Millikan, California Institute of Technology.

No. 8 to Dr. R. T. Knapp, California Institute of Technology.

No. 9 to Dr. L. G. Dunn, California Institute of Technology.

No. 10 to Mr. R. E. Jackson, Research Division, United Shoe Machinery Corporation, Boston, Mass.

No. 11 to Mr. F. L. Snyder, Westinghouse Ordnance Division, Westinghouse Electric & Mfg. Co., Sharon, Penn.

No. 12 to British Army Staff, British Ministry of Supply Mission, Washington, D.C., through: ATSC Classified Data and International Branch.